

# Geophysical Research Letters®



## RESEARCH LETTER

10.1029/2025GL116021

## Investigating Characteristic Droplet Size Distributions in Large Eddy Simulations of Stratocumulus Clouds

### Key Points:

- Characteristic droplet size distributions are identified for simulated stratocumulus clouds with Lagrangian and bin microphysics schemes
- Distributions are closely localized with the internal cell structure of convection and are more pronounced in the bin microphysics case
- Large-eddy scale clustering is observed, but across larger scales clusters are similar, lacking the variability seen in clouds from ACE-ENA

### Supporting Information:

Supporting Information may be found in the online version of this article.

### Correspondence to:

R. A. Shaw and N. Allwayin,  
rashaw@mtu.edu;  
nallwayi@mtu.edu

### Citation:

Allwayin, N., Miller, D. J., Chandrakar, K. K., Larsen, M. L., & Shaw, R. A. (2025). Investigating characteristic droplet size distributions in large eddy simulations of stratocumulus clouds. *Geophysical Research Letters*, 52, e2025GL116021. <https://doi.org/10.1029/2025GL116021>

Received 20 MAR 2025

Accepted 3 OCT 2025

### Author Contributions:

**Conceptualization:** Nithin Allwayin, Daniel J. Miller, Kamal Kant Chandrakar, Raymond A. Shaw

**Formal analysis:** Nithin Allwayin, Daniel J. Miller, Kamal Kant Chandrakar, Michael L. Larsen, Raymond A. Shaw

**Funding acquisition:** Raymond A. Shaw

**Methodology:** Nithin Allwayin, Daniel J. Miller, Kamal Kant Chandrakar, Michael L. Larsen, Raymond A. Shaw

**Software:** Nithin Allwayin, Daniel J. Miller, Kamal Kant Chandrakar

**Supervision:** Raymond A. Shaw

© 2025. The Author(s).

This is an open access article under the terms of the [Creative Commons Attribution-NonCommercial-NoDerivs License](#), which permits use and distribution in any medium, provided the original work is properly cited, the use is non-commercial and no modifications or adaptations are made.

Nithin Allwayin<sup>1,2</sup> , Daniel J. Miller<sup>3,4</sup> , Kamal Kant Chandrakar<sup>5</sup> , Michael L. Larsen<sup>1,6</sup> , and Raymond A. Shaw<sup>1</sup> 

<sup>1</sup>Department of Physics, Michigan Technological University, Houghton, MI, USA, <sup>2</sup>Now at, School of Marine and Atmospheric Sciences, Stony Brook University, Stony Brook, NY, USA, <sup>3</sup>Climate and Radiation Laboratory, NASA Goddard Space Flight Center, Greenbelt, MD, USA, <sup>4</sup>GESTAR-II, University of Maryland, Baltimore, MD, USA, <sup>5</sup>Mesoscale & Microscale Meteorology Laboratory, NSF National Center for Atmospheric Research, Boulder, CO, USA, <sup>6</sup>Department of Physics and Astronomy, College of Charleston, Charleston, SC, USA

**Abstract** Cloud processes relevant to radiative and precipitation properties depend on the shape of the cloud droplet size distribution. Recent holographic observations revealed that cloud droplet populations do not have the same size distribution shapes throughout but form regions of characteristic distributions with similar microphysical properties. We investigate the existence and properties of these characteristic distributions within Large-Eddy Simulations of stratocumulus clouds using Lagrangian and bin microphysics schemes. Distribution types are identified, revealing localized characteristic distributions that vary on the scale of the largest convective cell for simulations with bin microphysics. The results from the Lagrangian microphysics scheme hint at similar behavior. Compared to observations, the simulated clouds are much more uniform. Analysis of the LES results suggests a connection to the local entrainment rate, so the poorly resolved entrainment interface in LES may be a cause of the uniformity. The uniformity of the large-scale forcing could also be a factor.

**Plain Language Summary** The sizes of cloud droplets determine the amount of light scattered from clouds and the rate of formation of precipitation in clouds. How to represent droplet size distributions in numerical weather and climate models remains one of the largest sources of uncertainty in model predictions. Recent holographic measurements of droplet sizes within stratocumulus clouds suggest that the cloud droplet populations are not uniform across the cloud; rather, clouds contain regions of similar-looking droplet size distributions, each having distinct distribution shapes. Here we examine high-resolution simulations of these cloud systems using the same analytical approach and identify the existence of similar-looking droplet populations. We find that in the current output of these simulations, we do not observe the same variability in droplet sizes as seen for real clouds. However, the results point out that the characteristic shapes might be a good indicator of the physics in the individual convective cells.

## 1. Introduction

Clouds, particularly warm low-level stratocumulus clouds, play an essential role in Earth's energy budget (Slingo, 1990; Wood, 2012). How extensive and bright these clouds are determines the net cooling effect, making them extremely important in future global climate predictions (Dufresne & Bony, 2008; Stephens, 2005). The microphysical (droplet-scale) processes modulated by aerosols and turbulence are coupled to the large-scale cloud organization, lifetime, and properties (Chandrakar, Morrison, & Witte, 2022; Glassmeier et al., 2021; Kazil et al., 2017). These processes remain unresolved in model simulations, and inadequacies in their parametric representations contribute significantly to the uncertainties associated with cloud processes (Grabowski et al., 2019; Hu & Igel, 2024; Randall et al., 2003).

Currently, most bulk cloud model parameterizations assume an analytic shape for the cloud droplet size distribution (Khairoutdinov & Kogan, 2000; Liu & Daum, 2004; Liu et al., 2023; Morrison & Gettelman, 2008). In situ measurements of average cloud droplet size distributions inform these parametric representations (Miles et al., 2000). Higher order moments of these distributions are used in calculations of processes like collisions, drizzle formation, etc, and hence dictate the precipitation and radiative effects of the cloud (Covert et al., 2022; Long, 1974; Shaw, 2003). These mean representations often fail to fully capture the sub-grid scale variability in microphysical properties (Zhang et al., 2024). Recent field measurements utilizing holographic measurements of cloud droplet size distributions at cm-scales (Fugal et al., 2004; Fugal & Shaw, 2009; Spuler & Fugal, 2011) from

**Writing – original draft:**

Nithin Allwayin, Daniel J. Miller, Kamal Kant Chandrakar, Raymond A. Shaw

**Writing – review & editing:**

Nithin Allwayin, Daniel J. Miller, Kamal Kant Chandrakar, Michael L. Larsen, Raymond A. Shaw

the Aerosol and Cloud Experiments in the Eastern North Atlantic (ACE-ENA) field campaign (Wang et al., 2022) revealed that local droplet size distributions (DSDs) in stratocumulus clouds are narrow and do not resemble the bulk averaged droplet size distributions at larger spatial scales (Allwayin et al., 2024). Instead, they form characteristic distribution shapes resulting from similar cloud droplet populations residing in km-scale zones. Within cloud transects spanning 30–60 km, analogous to the typical grid box length scales in climate models, multiple such characteristic distribution types were found to exist. Additionally, these characteristic distribution modes span a range of diameters and only converge to the expected gamma distribution shape when aggregated over all the characteristic distributions within the coarser grid-scales (Ref Figure 1 in Allwayin et al. (2024)). These insights show that characteristic distributions offer a new way to characterize the sub-grid scale unresolved cloud processes.

This naturally leads us to ask whether such characteristic distribution types exist for the high-resolution Large Eddy Simulations often used to constrain and parameterize unresolved cloud processes in global climate models. This motivates the present investigation to determine if simulation outputs show the same variability and structure in cloud droplet size distributions as measured data. For this study, we utilized simulations of nocturnal stratocumulus clouds initialized based on observations and soundings made during the DYNAMICS and CHEMISTRY OF MARINE STRATOCUMULUS (DYCOMS-II) field campaign. The automated algorithm defined in Allwayin et al. (2022) is used to determine if these LES cloud fields have characteristic droplet size distribution shapes. It takes droplet size distribution data from a set of grid points in the simulations and outputs the subset that forms characteristic distributions (if any). Here, the algorithm is modified to deal with the large data volume of the LES cloud fields, as described in Section 2.

It is important to specify that the scope of this work is to determine the existence of characteristic distributions and lay a framework to set up further simulations and study. The paper is organized as follows. Section 2 discusses the details of the setup for the modifications made to the algorithm when applied to LES data. This is followed by the results and discussions in Section 3, and a summary of the key points is made in the concluding Section 4.

## 2. Materials and Methods

### 2.1. Large-Eddy Simulations

The Large-Eddy Simulations (LES) simulations in this study are initialized based on field campaign observations of marine stratocumulus clouds from the DYNAMICS and CHEMISTRY OF MARINE STRATOCUMULUS (DYCOMS-II) field campaign (research flight RF02). These simulations model nocturnal drizzling marine stratocumulus under a dry inversion. The cloud fields generated by the LESs in this study implement different microphysics schemes: bin-resolved microphysics and Lagrangian super-droplet microphysics schemes. The DHARMA LES model as defined in Ackerman et al. (2009) implements the bin-resolved microphysics with 25 logarithmically distributed DSD bins. This case employs a domain size of  $6.4 \times 6.4 \times 1.5$  km, with horizontal grid spacing of  $\Delta x = \Delta y = 50$  m and a stretched vertical grid with minimum spacing of 5 m to better resolve the temperature inversion (cloud top). The Lagrangian microphysics scheme (SDM, Shima et al., 2009), implemented within the Cloud Model 1 (CM1) LES dynamics core (Bryan & Fritsch, 2002), is also configured according to the setup in Ackerman et al. (2009). This setup uses a domain of  $50 \text{ km} \times 25 \text{ km} \times 1.5 \text{ km}$  with uniform grid spacings of 100 m (horizontal) and 5 m (vertical). The Lagrangian microphysics configuration applies a uniform forcing, with initial winds and large-scale shear set to zero, and the aerosol concentration is reduced by a factor of two (more details in the Supplement).

The input size distributions to the algorithm are derived from a horizontal layer at a snapshot of simulation time during the LES. This layer corresponds to a constant altitude in the cloud layer, and thus aims to gain insights into the 2-D spatial variability and organization of the characteristic drop size distribution types. The horizontal layers are chosen at multiple altitudes corresponding to the cloud base, core, and top regions to cover different processes governing the DSD shape. Additionally, simulations at multiple time steps are also analyzed, corresponding to times before and after the onset of drizzle (see Table S1 in Supporting Information S1).

For simulations with bin microphysics schemes, the distributions within each grid box are the input for the algorithm. For the Lagrangian case, however, the super-droplets from 4 horizontally adjacent grid cells are combined to form one local DSD. This is done to ensure there are enough super droplets ( $>100$ ) in each sample to form a reasonably smooth size distribution. Also, the effective resolution for these LES models due to their

numerical schemes is of the order of a few grid cells (e.g., see Figure 3 in Grabowski et al. (2025)), so little information is lost by combining these grids. The single-layer array of distributions is then input into the algorithm to identify characteristic distribution shapes.

## 2.2. Algorithm: Clustering Similar Droplet Size Distributions

The algorithm searches through the input size distributions and then determines a set of characteristic distribution types that exist for the input data. The algorithm works by uniquely combining hypothesis testing with density-based clustering algorithms to determine clusters of similar size distribution types (Allwayin et al., 2022). The input data in our case is composed of size distributions of cloud droplets within each LES grid box. This array of droplet size distributions is fed into the algorithm, which then semi-automatically determines the number and shape of characteristic distributions. The first step in the algorithm is to compare two DSDs using the two-sample Kolmogorov-Smirnov (KS) test (Kendall & Stuart, 1979) to determine if they are samples from the same parent size distribution. This step is repeated for all the DSD pairs, and so a set of  $n$  distributions will have  $n^2$  results, which are arranged in the form of a matrix referred to hereafter as the KS matrix. The previous use of this algorithm does an ensemble of KS tests for each distribution pair by resampling the distribution to have a constant number concentration to eliminate artifacts from dissimilar sample sizes (Glienke et al., 2020). Here we replace this step by doing a single KS test for each distribution pair and utilize the p-value score as the indicator of the similarity in the KS matrix. In this context, the p-value offers a computationally efficient measure of how much the data supports similarity between distributions; for a fuller discussion on comparison with the ensemble KS tests, see the Supplement.

Only samples containing cloud droplets above a cutoff value of 70% of the mean droplet count value are utilized in the analysis. Subsequently, the density-based clustering algorithm—Ordering Points To Identify the Clustering Structure (OPTICS) (Ankerst et al., 1999) is then used on the KS matrix. The OPTICS algorithm scans the similarity scores (in this study, p-values) in each row of the KS matrix and uses them to link it to other rows. Each row represents one input size distribution and the collection of these linked rows is the collection of DSDs that form the characteristic distribution for that cluster.

The other change to the previous implementation of the algorithm is in the format of the input size distributions. For previously used holographic data, sizes for all individual cloud droplets were available. These individual droplet sizes are input to the *kstest2* function (in MATLAB), which then calculates the empirical cumulative distribution function (CDF) to test the similarity between two DSDs. However, this information is not available for the LES. The bin scheme provides droplet counts within specific diameter bins, and the super droplets include a multiplicity factor for all droplets, making it comparable to having a specific number of droplets at each of these diameters. The KS function is modified to input the binned size distribution directly instead of the individual droplet diameters. These distributions are converted to CDFs for the KS test. For the super droplets, we bin into uniform 2  $\mu\text{m}$  bins from the Lagrangian droplet framework to make it better suited for comparisons to the bin scheme. Even after combining 4 grids, the DSDs from the super-droplets are noisy. The MATLAB function *smooth*, which applies a moving average, is used to get a smoother DSD for use in the clustering algorithm.

For the CDFs used in the KS comparisons, the mean diameter of each bin determines the step locations, and the droplet counts in these bins define the step heights. This means that the number of steps in the CDF is based on the total number of bins, rather than the actual droplet counts, as would be the case when constructing an empirical CDF. The KS test is known to be sensitive to this number of droplets in the sample (Glienke et al., 2020); to account for this, we include an additional tunable parameter to set this number. The second parameter input to the algorithm is the minimum number of input size distributions required to form one characteristic size distribution. Additional details regarding the algorithm can be found in Allwayin et al. (2022).

## 3. Results

### 3.1. Analysis of Characteristic Droplet Size Distributions From LES

Characteristic distributions are identified by the algorithm for the cloud DSDs from both bin and Lagrangian LES frameworks. An illustration of these distribution clusters for the bin microphysics case is shown in Figure 1a. The number of input distributions associated with an LES horizontal layer is  $\approx 17000$  for the bin and  $\approx 31000$  for the Lagrangian super droplet case, respectively. The algorithm parameters are tuned to distinguish small differences

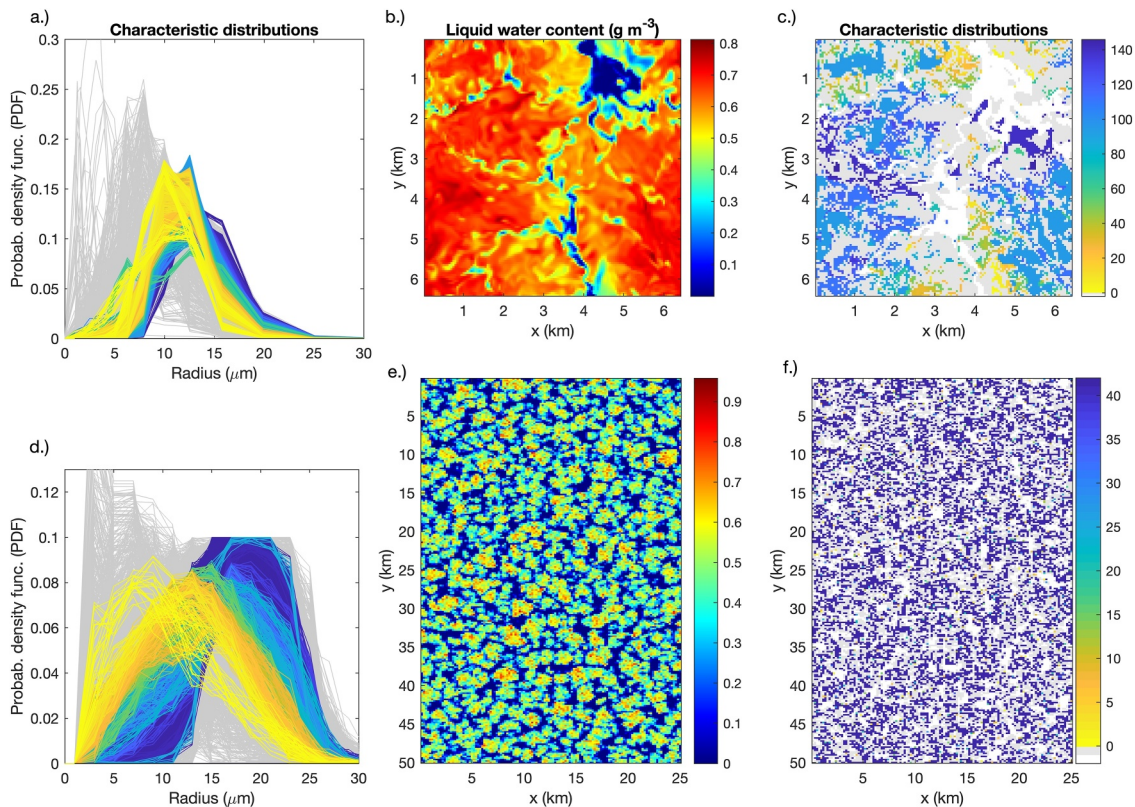


**Figure 1.** (a) Probability density functions of the different clusters, (b) Liquid water content, (c) characteristic distributions, for a horizontal slice across the core of the cloud in the DHARMA LES with spectral bin microphysics. The different colors represent the characteristic distributions in the increasing order of effective radius. Gray marks the regions not identified with any of the clusters by the algorithm. White marks the region below the cutoff and is not considered for analysis. Panels (d–f) show the same quantities as in (a–c), but for the LES with Lagrangian super-droplets.

and therefore the number of characteristic distributions identified is often large ( $\geq 100$ ) for these cases. This is desirable, as the objective of the study is to understand correlations and trends for the distribution types. For the case illustrated in Figure 1a, around 147 characteristic size distributions were identified. To better visualize these characteristic DSDs, they are colored in the increasing order of mean radius (with yellow depicting the smallest values). Gray lines mark the distributions marked as not belonging to any of the characteristic DSDs by the algorithm.

Using the characteristic DSDs offers a unique perspective to understand the internal structure of a convective cell. As shown in Figure 1a, the characteristic distributions are identified for a horizontal slice at about the 75% level of cloud thickness, from the top of the LES domain for the bin microphysics scheme. This single layer of the cloud is displayed from a top-down view of the liquid water content fields. This slice is taken from the core of the cloud profile after the onset of drizzle formation (Figure 1b). The spatial distribution of the characteristic DSDs exhibits coherent localized structure (Figure 1c) similar to the field data. The colors correspond to the characteristic DSDs in Figure 1a. The gray regions indicate DSDs that were not identified and clustered into any characteristic distributions. These are largely associated with regions closer to cloud holes. We see that the characteristic DSDs with smaller mean radius (yellow DSDs) are slightly narrower compared to the larger radius ones (see also Table 1 and Figure S1 in Supporting Information S1). This is perhaps the first hint at broader relationships between characteristic distributions and bulk microphysical properties.

Correlations between characteristic distributions and bulk cloud properties of interest are shown in Figure 2. The results here are for the same microphysical and dynamic fields presented in Figures 1a–1c. Figure 2a shows the drizzle-dominated regions in the LES domain. These are regions with greater contribution from cloud droplets above  $40 \mu\text{m}$  in diameter. The drizzle-dominated regions can be visually identified with the characteristic DSDs with the larger radius. Surprisingly, such distinctions are not obvious from the total liquid water content fields.

**Table 1**

*Droplet Size Distribution Properties From Holographic Detector for Clouds (HOLODEC) During ACE-ENA and Large Eddy Simulations (Bin-Resolved and Lagrangian Microphysics) for DYCOMS-II*

Data set	Length scales (km)	Mode diameters ( $\mu\text{m}$ )	Standard deviation ( $\mu\text{m}$ )
HOLODEC-IOP1-RF18	2.6, 1.9, 0.7, 1.8, 1.6, 1.1	22.1, 21.3, 19.8, 14.4, 13.5, 13.4	4.3, 3.4, 3.4, 3.9, 3.8, 3.5
DHARMA LES: bin-resolved microphysics	3.7, 0.8, 0.6, 0.7, 4.2, 0.6, 2.3, 0.5, 0.5, 0.5, 0.6, 0.7, 0.7, 0.6, 0.6, 0.5, 0.7, 0.5, 0.5	25.4, 25.4, 25.4, 25.4, 25.4, 25.4, 25.9, 25.4, 25.4, 25.4, 25.4, 25.4, 25.4, 25.4, 25.4, 25.4, 25.4, 25.4	6.4, 6.9, 7.3, 5.7, 4.7, 5.3, 7.6, 6.9, 4.2, 7.5, 7.4, 5.9, 5.7, 5.2, 5.0, 5.5, 6.3, 6.6, 8.9
Cloud Model 1 LES: Lagrangian super-droplet method	12.7	33.9	8.3

*Note.* Only characteristic distributions exceeding 500 m are included.

This relationship between drizzle and total liquid water is shown in Figure 2b. Each point corresponds to an individual grid point and is colored according to identified characteristic distributions. There is a clear demarcation between the characteristic DSDs with the drizzle amount, but such distinctions are not obvious between the least and most diluted regions. Interestingly, these drizzle-dominated regions also appear close to the more turbulent and subsiding regions of the cloud, as seen in Figure 2c. The lower mean radius and slightly narrow distributions appear predominantly in the updraft regions of the cloud. The larger radius distributions are also the

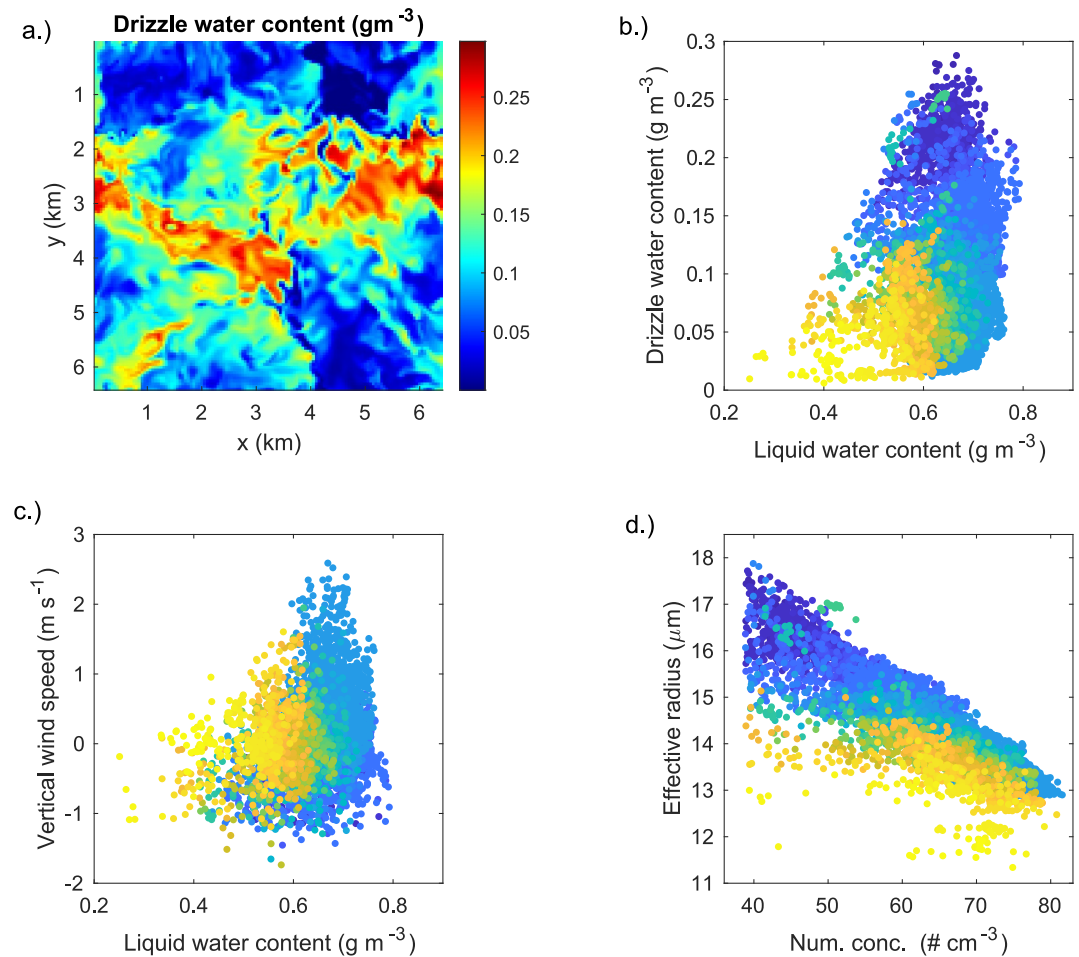


**Figure 2.** (a) Drizzle water content and correlation plots between (b) liquid and drizzle water contents, (c) liquid water content and vertical velocity, and (d) number concentration and effective radius for the DYCOMS-II bin case shown in Figures 1a–1c. The color schemes correspond to the characteristic distributions and are consistent with the previous figure.

ones with the smallest number concentrations (Figure 2d). These results indicate that characteristic distributions are connected to the physics of the convective cell and thus represent the coupling between microphysical and dynamic cloud properties.

An illustration of the characteristic distributions and the corresponding 2D distributions for LES models with Lagrangian microphysics scheme is shown in Figures 1d–1f. This snapshot is from a time before drizzle formation. Note that here the domain dimensions are 10 and 5 times larger than those in the bin-resolved microphysics simulations. We observe the cloud DSDs to be very uniform with relatively little large-scale spatial difference. The observed uniformity across the larger domain could potentially be from the uniform boundary forcing, the uniformity of the aerosol distribution, or the lack of vertical wind shear. Most notably, the entrainment interfacial layer is not fully resolved, and therefore, the local variability of entrainment processes may not be fully represented. The difference to clouds from ACE-ENA is striking (refer to Figure 1 in Allwayin et al. (2024)), where characteristic distributions were found to scale with circulation-cell sizes. The entrainment rates for the ACE-ENA case also varied across similar spatial scales (Yeom et al., 2024). It is worth considering what is missed by using such idealized simulations that lack large-scale structure to develop sub-grid-scale parameterizations for models, when in fact much more microphysical structure exists in real stratocumulus clouds.

In addition, we find that when compared to the bin microphysics case, there is less variability not only across the simulation domain but also within each convective cell in the Lagrangian microphysics case. This could result from the low super droplet counts and the subsequently applied numerical smoothing. Ideally, the analysis technique as applied requires 4 times the current super droplet counts–equivalent to combining 16 grid cells in the current setup, which would mean averaging all the microphysical variability within a convective cell.

### 3.2. Comparison to Field Observations

Characteristic distributions observed in these idealized LES runs lack the large-scale spatial variability observed in the holographic data from the ACE-ENA field campaign. Though the LES runs are not specifically set up for ACE-ENA, it is insightful to compare the properties of characteristic distributions to the field data. Specifically, consider the 60-km cloud segment from research flight RF18, highlighted in Figures 1–3 in Allwayin et al. (2024). We determine the characteristic length scales, mode diameter, and standard deviation of droplet sizes for the most prevalent clusters from the holographic and LES data for comparison. The Lagrangian microphysics simulations are better suited for comparison to the field data, as their domain length is around 50 km. For the Lagrangian LES case shown in Figures 1d–1f, there is one dominant characteristic distribution with a length scale of around 13 km, a mode diameter of 34  $\mu\text{m}$ , and a standard deviation of 8  $\mu\text{m}$ . The holographic DSDs exhibit more microphysical variability with mode diameters  $\approx 13$ –23  $\mu\text{m}$ , and are also narrower with standard deviations of 4  $\mu\text{m}$  or below (see Table 1). This variability across different convective cells is not observed in the LES. For a much smaller domain size in the bin microphysics case (shown in Figures 1a–1c and 2), there are 19 major characteristic distributions. These distributions have a mode diameter around 25  $\mu\text{m}$  with the standard deviation varying from 4 to 9  $\mu\text{m}$ . Here too, the distributions lack the variability seen in the field results.

### 3.3. Characteristic DSDs and Entrainment

The characteristic droplet size distributions offer a unique tool for analyzing the complex relationships between cloud dynamics and microphysics. In essence, the characteristic distributions may be an indicator of physical processes that lead to their formation in the first place. To explore this possibility, we look at the possible connection between characteristic DSDs and the entrainment rate in the bin-resolved LES. We use a simulation snapshot early in cloud development, prior to precipitation onset, near the Entrainment Interfacial Layer (EIL) at the cloud top, as shown in Figure 3. This analysis is performed by sorting the characteristic distribution cluster index by median entrainment rate for each cluster. These features indicate a plausible causal relationship between entrainment in the EIL and the DSD shape evolution across the clustered characteristic DSD populations. Traditionally, the impact of entrainment mixing on cloud microphysics would be analyzed in the context of mixing diagrams. Such analyses have often struggled to clarify the impact of entrainment on microphysics (Burnet & Brenguier, 2007; Desai et al., 2021; Lehmann et al., 2009), possibly as a result of spatial averaging that mixes the microphysical signatures of different entrainment regimes (Yeom et al., 2023). By conditioning on the clustered DSDs, a clearer picture emerges that supports the important connection between size distribution shape and the local entrainment rate. Variability in entrainment rate is connected to local properties of the EIL due to

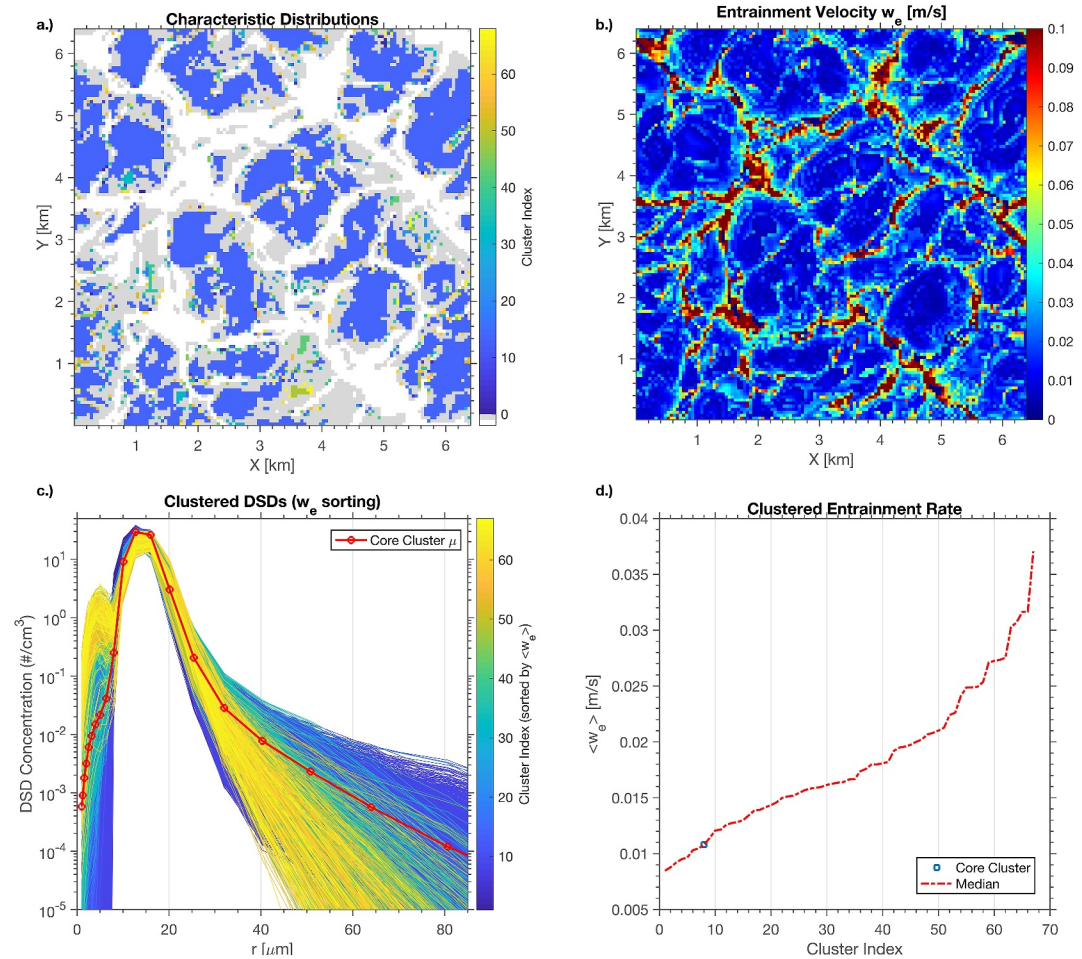


**Figure 3.** (a) Map of characteristic distribution clusters from the DHARMA bin-resolved LES for a horizontal slice within the Entrainment Interfacial Layer (EIL)- approximately 15 m below the mean cloud top. Cluster index is sorted by increasing median entrainment rate of each cluster. Regions in gray are unclustered, while regions in white are considered cloud-free in this layer. (b) Map of the entrainment rate at cloud top calculated using a jump-flux method. (c) DSD spaghetti plot displaying the transition of DSD shape with increasing entrainment rate (color indicates cluster index). (d) The median entrainment rate of each clustered DSD index within the sorted data set.

wind velocity shear (Katzwinkel et al., 2012; Kopec et al., 2016; La & Yum, 2024; Mellado et al., 2014; Yeom et al., 2024).

#### 4. Conclusions

This study aimed to investigate the existence of characteristic droplet size distributions within stratocumulus cloud fields simulated using LES using Lagrangian and bin microphysics schemes. An important finding of this study is that, though present, the behavior of characteristic distributions from the LESs differs substantially from the holographic field data from the Aerosol and Cloud Experiments in the Eastern North Atlantic (ACE-ENA) field campaign (Allwayin et al., 2024). In agreement with the campaign results, we find that there are prominent clusters of characteristic distributions on length scales of a boundary layer eddy. However, in contrast, we do not find that the identified characteristic distribution varies from one convective core to another, as it did in the field data set. This may be the result of uniform boundary forcings in these simulation configurations for the Lagrangian microphysics case or from spatial domain limitations for the bin microphysics case. In these scenarios, we do not expect to see such large differences across the simulation domain. The LES forcings are uniform and highly idealized, with assumptions such as uniform surface fluxes, no aerosol heterogeneity, and no applied horizontal advection tendencies.

We find that the variability in observed size distribution types within the LES with bin microphysics is correlated with the local entrainment rate. However, it is known that the entrainment interfacial layer is poorly resolved in most LES. This could explain why there is little variability in microphysical properties beyond that associated with the large boundary layer circulation/eddies. The identified characteristic distributions are spatially coherent and closely linked to the microphysical and dynamic fields in a way that single parameters like liquid water content or mean radii may not be. For entrainment studies, parameters like the mean radius have long been used to define and analyze mixing diagrams — despite the fact that a bulk DSD variable can hide more complex DSD responses (e.g., multi-modal DSD). To that end, a distribution clustering tool like this presents a unique and powerful tool for further analysis.

The results underscore the need to understand what physics is driving the greater microphysical variability in field observations compared to the simulations. The LESs used in this study are idealized cases, and additional processes can be explored in future studies. For example, understanding the role of horizontal gradients in aerosol concentrations could provide valuable insights. Simulations that better resolve the entrainment interfacial layer are also likely to yield insight. There is greater potential to develop the Lagrangian LES analysis, as it allows tracking the history of the droplets that form characteristic distributions. For the simulations, however, at least 4 times the super droplet counts are desirable.

Idealized large-eddy simulations inform cloud representations in coarse-resolution models. Their ability to resolve boundary layer eddies makes them extremely useful; however, the microphysics schemes have numerical diffusion or small-number fluctuations, and we need to be cautious of their ability to capture the intricate feedbacks and relationships observed in real clouds. For example, cloud measurements have shown large-eddy scale variability in entrainment rates (Yeom et al., 2024) comparable to the characteristic distribution length scales observed from ACE-ENA. For these model simulations, the entrainment interfacial layer (EIL) and its variability is not fully resolved, and our results suggest this could be a reason for the relative uniformity. A higher-resolution simulation that explicitly captures the EIL, and with large numbers of Lagrangian superparticles to faithfully capture microphysical variability, would be ideal for determining the extent to which local entrainment characteristics vary significantly and to better understand the causal relationships between entrainment and the cloud droplet size distribution.

### Conflict of Interest

The authors declare no conflicts of interest relevant to this study.

### Data Availability Statement

The Large Eddy Simulation data sets used in this study have been described and can be accessed as detailed in Miller et al. (2016) and Chandrakar, Morrison, and Witte (2022). The KS-ML clustering algorithm is documented in Allwayin et al. (2022).

### References

- Ackerman, A. S., van Zanten, M. C., Stevens, B., Savic-Jovicic, V., Bretherton, C. S., Chlond, A., et al. (2009). Large-eddy simulations of a drizzling, stratocumulus-topped marine boundary layer. *Monthly Weather Review*, 137(3), 1083–1110. <https://doi.org/10.1175/2008MWR2582.1>
- Allwayin, N., Larsen, M. L., Glienke, S., & Shaw, R. A. (2024). Locally narrow droplet size distributions are ubiquitous in stratocumulus clouds. *Science*, 384(6695), 528–532. <https://doi.org/10.1126/science.adi5550>
- Allwayin, N., Larsen, M. L., Shaw, A. G., & Shaw, R. A. (2022). Automated identification of characteristic droplet size distributions in stratocumulus clouds utilizing a data clustering algorithm. *Artificial Intelligence for the Earth Systems*, 1(3), e220003. <https://doi.org/10.1175/AIES-D-22-0003.1>
- Ankerst, M., Breunig, M. M., Kriegl, H.-P., & Sander, J. (1999). OPTICS: Ordering Points to Identify the Clustering Structure. *SIGMOD Rec.*, 28(2), 49–60. <https://doi.org/10.1145/304181.304187>
- Bryan, G. H., & Fritsch, J. M. (2002). A benchmark simulation for moist nonhydrostatic numerical models. *Monthly Weather Review*, 130(12), 2917–2928. [https://doi.org/10.1175/1520-0493\(2002\)130<2917:absfmm>2.0.co;2](https://doi.org/10.1175/1520-0493(2002)130<2917:absfmm>2.0.co;2)
- Burnet, F., & Brenguier, J.-L. (2007). Observational study of the entrainment-mixing process in warm convective clouds. *Journal of the Atmospheric Sciences*, 64(6), 1995–2011. <https://doi.org/10.1175/JAS3928.1>
- Chandrakar, K. K., Morrison, H., & Witte, M. (2022b). Evolution of droplet size distributions during the transition of an ultraclean stratocumulus cloud system to open cell structure: An les investigation using lagrangian microphysics. *Geophysical Research Letters*, 49(17), e2022GL100511. <https://doi.org/10.1029/2022GL100511>
- Covert, J. A., Mechem, D. B., & Zhang, Z. (2022). Subgrid-scale horizontal and vertical variation of cloud water in stratocumulus clouds: A case study based on les and comparisons with in situ observations. *Atmospheric Chemistry and Physics*, 22(2), 1159–1174. <https://doi.org/10.5194/acp-22-1159-2022>

### Acknowledgments

This research was supported by the US Department of Energy's Atmospheric System Research, an Office of Science Biological and Environmental Research program, under DESC0020053 (R.A.S.) and through the National Science Foundation awards AGS-2019649 (R.A.S.) and AGS-2001490 (M.L.L.). Contribution of DHARMA LES and analysis was supported by NASA's PACE Science Team, NNH23ZDA001N-PACE (D.J.M.). Contributions from K.K.C. were supported by the NSF National Center for Atmospheric Research, which is a major facility sponsored by the U.S. National Science Foundation under Cooperative Agreement No. 1852977. N. Allwayin thanks NASA and NCAR for supporting collaborative visits that fostered progress on this research.

- Desai, N., Liu, Y., Glienke, S., Shaw, R. A., Lu, C., Wang, J., & Gao, S. (2021). Vertical variation of turbulent entrainment mixing processes in marine stratocumulus clouds using high-resolution digital holography. *Journal of Geophysical Research*, 126(7), e2020JD033527. <https://doi.org/10.1029/2020jd033527>
- Dufresne, J.-L., & Bony, S. (2008). An assessment of the primary sources of spread of global warming estimates from coupled atmosphere–ocean models. *Journal of Climate*, 21(19), 5135–5144. <https://doi.org/10.1175/2008JCLI2239.1>
- Fugal, J. P., & Shaw, R. A. (2009). Cloud particle size distributions measured with an airborne digital in-line holographic instrument. *Atmospheric Measurement Techniques*, 2(1), 259–271. <https://doi.org/10.5194/amt-2-259-2009>
- Fugal, J. P., Shaw, R. A., Saw, E. W., & Sergeyev, A. V. (2004). Airborne digital holographic system for cloud particle measurements. *Applied Optics*, 43(32), 5987–5995. <https://doi.org/10.1364/AO.43.005987>
- Glassmeier, F., Hoffmann, F., Johnson, J. S., Yamaguchi, T., Carslaw, K. S., & Feingold, G. (2021). Aerosol-cloud-climate cooling overestimated by ship-track data. *Science*, 371(6528), 485–489. <https://doi.org/10.1126/science.abd3980>
- Glienke, S., Kostinski, A. B., Shaw, R. A., Larsen, M. L., Fugal, J. P., Schlenker, O., & Borrmann, S. (2020). Holographic observations of centimeter-scale nonuniformities within marine stratocumulus clouds. *Journal of the Atmospheric Sciences*, 77(2), 499–512. <https://doi.org/10.1175/JAS-D-19-0164.1>
- Grabowski, W. W., Chandrakar, K. K., & Morrison, H. (2025). Untangling the broadening of adiabatic cloud droplet spectra through eddy hopping in a high-resolution cumulus congestus simulation. *Journal of the Atmospheric Sciences*, 82(8), 1585–1599. <https://doi.org/10.1175/JAS-D-25-0003.1>
- Grabowski, W. W., Morrison, H., Shima, S.-I., Abade, G. C., Dziekan, P., & Pawlowska, H. (2019). Modeling of cloud microphysics: Can we do better? *Bulletin of the American Meteorological Society*, 100(4), 655–672. <https://doi.org/10.1175/BAMS-D-18-0005.1>
- Hu, A. Z., & Igel, A. L. (2024). Bulk microphysics schemes May perform better with a unified cloud-rain category. *Journal of Advances in Modeling Earth Systems*, 16(7), e2023MS004068. <https://doi.org/10.1029/2023MS004068>
- Katzwinkel, J., Siebert, H., & Shaw, R. (2012). Observation of a self-limiting, shear-induced turbulent inversion layer above marine stratocumulus. *Boundary-Layer Meteorology*, 145(1), 131–143. <https://doi.org/10.1007/s10546-011-9683-4>
- Kazil, J., Yamaguchi, T., & Feingold, G. (2017). Mesoscale organization, entrainment, and the properties of a closed-cell stratocumulus cloud. *Journal of Advances in Modeling Earth Systems*, 9(5), 2214–2229. <https://doi.org/10.1002/2017MS001072>
- Kendall, M., & Stuart, A. (1979). *The advanced theory of statistics* (Vol. 2). Charles Griffin.
- Khairoutdinov, M., & Kogan, Y. (2000). A new cloud physics parameterization in a large-eddy simulation model of marine stratocumulus. *Monthly Weather Review*, 128(1), 229–243. [https://doi.org/10.1175/1520-0493\(2000\)128<0229:ANCPPI>2.0.CO;2](https://doi.org/10.1175/1520-0493(2000)128<0229:ANCPPI>2.0.CO;2)
- Kopec, M. K., Malinowski, S. P., & Piotrowski, Z. P. (2016). Effects of wind shear and radiative cooling on the stratocumulus-topped boundary layer. *Quarterly Journal of the Royal Meteorological Society*, 142(701), 3222–3233. <https://doi.org/10.1002/qj.2903>
- La, I., & Yum, S. S. (2024). Relationship between vertical variation of cloud microphysical properties and thickness of the entrainment interfacial layer in physics of stratocumulus top stratocumulus clouds. *Quarterly Journal of the Royal Meteorological Society*, 150(765), 5037–5056. <https://doi.org/10.1002/qj.4855>
- Lehmann, K., Siebert, H., & Shaw, R. A. (2009). Homogeneous and inhomogeneous mixing in cumulus clouds: Dependence on local turbulence structure. *Journal of the Atmospheric Sciences*, 66(12), 3641–3659. <https://doi.org/10.1175/2009JAS3012.1>
- Liu, Y., & Daum, P. (2004). Parameterization of the autoconversion process. Part I: Analytical formulation of the Kessler-type parameterizations. *Journal of the Atmospheric Sciences*, 61(13), 1539–1548. [https://doi.org/10.1175/1520-0469\(2004\)061<1539:POTAPI>2.0.CO;2](https://doi.org/10.1175/1520-0469(2004)061<1539:POTAPI>2.0.CO;2)
- Liu, Y., Yau, M.-K., Shima, S.-I., Lu, C., & Chen, S. (2023). Parameterization and explicit modeling of cloud microphysics: Approaches, challenges, and future directions. *Advances in Atmospheric Sciences*, 40(5), 747–790. <https://doi.org/10.1007/s00376-022-2077-3>
- Long, A. B. (1974). Solutions to the droplet collection equation for polynomial kernels. *Journal of the Atmospheric Sciences*, 31(4), 1040–1052. [https://doi.org/10.1175/1520-0469\(1974\)031<1040:STTDCE>2.0.CO;2](https://doi.org/10.1175/1520-0469(1974)031<1040:STTDCE>2.0.CO;2)
- Mellado, J. P., Stevens, B., & Schmidt, H. (2014). Wind shear and buoyancy reversal at the top of stratocumulus. *Journal of the Atmospheric Sciences*, 71(3), 1040–1057. <https://doi.org/10.1175/jas-d-13-0189.1>
- Miles, N. L., Verlinde, J., & Clothiaux, E. E. (2000). Cloud droplet size distributions in low-level stratiform clouds. *Journal of the Atmospheric Sciences*, 57(2), 295–311. [https://doi.org/10.1175/1520-0469\(2000\)057<0295:CDSIDL>2.0.CO;2](https://doi.org/10.1175/1520-0469(2000)057<0295:CDSIDL>2.0.CO;2)
- Miller, D. J., Zhang, Z., Ackerman, A. S., Platnick, S., & Baum, B. A. (2016). The impact of cloud vertical profile on liquid water path retrieval based on the bispectral method: A theoretical study based on large-eddy simulations of shallow marine boundary layer clouds. *Journal of Geophysical Research: Atmospheres*, 121(8), 4122–4141. <https://doi.org/10.1002/2015JD024322>
- Morrison, H., & Gettelman, A. (2008). A new two-moment bulk stratiform cloud microphysics scheme in the Community Atmosphere Model, version 3 (CAM3). Part I: Description and numerical tests. *Journal of Climate*, 21(15), 3642–3659. <https://doi.org/10.1175/2008JCLI2105.1>
- Randall, D., Khairoutdinov, M., Arakawa, A., & Grabowski, W. (2003). Breaking the cloud parameterization deadlock. *Bulletin of the American Meteorological Society*, 84(11), 1547–1564. <https://doi.org/10.1175/BAMS-84-11-1547>
- Shaw, R. A. (2003). Particle-turbulence interactions in atmospheric clouds. [Journal Article]. *Annual Review of Fluid Mechanics*, 35(1), 183–227. <https://doi.org/10.1146/annurev.fluid.35.101101.161125>
- Shima, S.-i., Kusano, K., Kawano, A., Sugiyama, T., & Kawahara, S. (2009). The super-droplet method for the numerical simulation of clouds and precipitation: A particle-based and probabilistic microphysics model coupled with a non-hydrostatic model. *Quarterly Journal of the Royal Meteorological Society: A journal of the atmospheric sciences, applied meteorology and physical oceanography*, 135(642), 1307–1320. <https://doi.org/10.1002/qj.441>
- Slingo, A. (1990). Sensitivity of the Earth's radiation budget to changes in low clouds. *Nature*, 343(6253), 49–51. <https://doi.org/10.1038/343049a0>
- Spuler, S. M., & Fugal, J. (2011). Design of an in-line, digital holographic imaging system for airborne measurement of clouds. *Applied Optics*, 50(10), 1405–1412. <https://doi.org/10.1364/AO.50.001405>
- Stephens, G. L. (2005). Cloud feedbacks in the climate system: A critical review. *Journal of Climate*, 18(2), 237–273. <https://doi.org/10.1175/JCLI-3243.1>
- Wang, J., Wood, R., Jensen, M. P., Chiu, J. C., Liu, Y., Lamer, K., et al. (2022). Aerosol and Cloud Experiments in the Eastern North Atlantic (ACE-ENA). *Bulletin of the American Meteorological Society*, 103(2), E619–E641. <https://doi.org/10.1175/BAMS-D-19-0220.1>
- Wood, R. (2012). Stratocumulus clouds. *Monthly Weather Review*, 140(8), 2373–2423. <https://doi.org/10.1175/MWR-D-11-00121.1>
- Yeom, J. M., Helman, I., Prabhakaran, P., Anderson, J. C., Yang, F., Shaw, R. A., & Cantrell, W. (2023). Cloud microphysical response to entrainment and mixing is locally inhomogeneous and globally homogeneous: Evidence from the lab. *Proceedings of the National Academy of Sciences*, 120(42), e2307354120. <https://doi.org/10.1073/pnas.2307354120>

- Yeom, J. M., Szodry, K.-E., Siebert, H., Ehrlich, A., Mellado, J. P., Shaw, R. A., & Yum, S. S. (2024). High-resolution measurements of microphysics and entrainment in marine stratocumulus clouds. *Quarterly Journal of the Royal Meteorological Society*, *150*(758), 81–97. <https://doi.org/10.1002/qj.4586>
- Zhang, Z., Mechem, D. B., Chiu, J. C., & Covert, J. A. (2024). A comprehensive analysis of uncertainties in warm-rain parameterizations in climate models based on in situ measurements. *Journal of the Atmospheric Sciences*, *81*(7), 1251–1269. <https://doi.org/10.1175/JAS-D-23-0198.1>

## References From the Supporting Information

- Ackerman, A. S., Kirkpatrick, M. P., Stevens, D. E., & Toon, O. B. (2004). The impact of humidity above stratiform clouds on indirect aerosol climate forcing. *Nature*, *432*(7020), 1014–1017. <https://doi.org/10.1038/nature03174>
- Chandrakar, K. K., Morrison, H., Grabowski, W. W., & Bryan, G. H. (2022a). Comparison of lagrangian super-droplet and Eulerian double-moment spectral microphysics schemes in large-eddy simulations of an isolated cumulus-congestus cloud. *Journal of the Atmospheric Sciences*, *79*(7), 1887–1910. <https://doi.org/10.1175/jas-d-21-0138.1>
- Chandrakar, K. K., Grabowski, W. W., Morrison, H., & Bryan, G. H. (2021). Impact of entrainment mixing and turbulent fluctuations on droplet size distributions in a cumulus cloud: An investigation using lagrangian microphysics with a subgrid-scale model. *Journal of the Atmospheric Sciences*, *78*(9), 2983–3005. <https://doi.org/10.1175/jas-d-20-0281.1>
- Deardorff, J. W. (1980). Stratocumulus-capped mixed layers derived from a three-dimensional model. *Boundary-Layer Meteorology*, *18*(4), 495–527. <https://doi.org/10.1007/bf00119502>
- Mellado, J.-P., Bretherton, C., Stevens, B., & Wyant, M. (2018). DNS and LES for simulating stratocumulus: Better together. *Journal of Advances in Modeling Earth Systems*, *10*(7), 1421–1438. <https://doi.org/10.1029/2018ms001312>
- Morrison, H., Witte, M., Bryan, G. H., Harrington, J. Y., & Lebo, Z. J. (2018). Broadening of modeled cloud droplet spectra using bin microphysics in an Eulerian spatial domain. *Journal of the Atmospheric Sciences*, *75*(11), 4005–4030. <https://doi.org/10.1175/jas-d-18-0055.1>
- Stevens, B., Moeng, C.-H., Ackerman, A. S., Bretherton, C. S., Chlond, A., de Roode, S., et al. (2005). Evaluation of large-eddy simulations via observations of nocturnal marine stratocumulus. *Monthly Weather Review*, *133*(6), 1443–1462. <https://doi.org/10.1175/mwr2930.1>
- Weil, J. C., Sullivan, P. P., & Moeng, C.-H. (2004). The use of large-eddy simulations in lagrangian particle dispersion models. *Journal of the Atmospheric Sciences*, *61*(23), 2877–2887. <https://doi.org/10.1175/jas-3302.1>
- Zhang, Z., Ackerman, A. S., Feingold, G., Platnick, S., Pincus, R., & Xue, H. (2012). Effects of cloud horizontal inhomogeneity and drizzle on remote sensing of cloud droplet effective radius: Case studies based on large-eddy simulations. *Journal of Geophysical Research*, *117*(D19). <https://doi.org/10.1029/2012JD017655>